

The Role of Surface Entropy in Statistical Emission of Massive Fragments from Equilibrated Nuclear Systems

Jan Töke, Jun Lu, and W.Udo Schröder

Department of Chemistry, University of Rochester, Rochester, New York 14627

(Dated: November 11, 2018)

Abstract

Statistical fragment emission from excited nuclear systems is studied within the framework of a schematic Fermi-gas model combined with Weisskopf's detailed balance approach. The formalism considers thermal expansion of finite nuclear systems and pays special attention to the role of the diffuse surface region in the decay of hot equilibrated systems. It is found that with increasing excitation energy, effects of surface entropy lead to a systematic and significant reduction of effective emission barriers for fragments and, eventually, to the vanishing of these barriers. The formalism provides a natural explanation for the occurrence of negative nuclear heat capacities reported in the literature. It also accounts for the observed linearity of pseudo-Arrhenius plots of the logarithm of the fragment emission probability *versus* the inverse square-root of the excitation energy, but does not predict true Arrhenius behavior of these emission probabilities.

PACS numbers: 21.65+f, 21.60.Ev, 25.70.Pq

I. INTRODUCTION

Over the last decade, a considerable effort has been made to understand the phenomenon of production of multiple intermediate-mass fragments (IMF) in individual nuclear reaction events. Yet, in spite of this effort, understanding of this process is still far from being satisfactory. For example, a consensus is still lacking on even such a fundamental issue of whether the fragment production is dominantly a statistical or a dynamical process. To a certain extent, such lack of consensus is due to the fact that different models, promoting conflicting production scenarios, appear equally successful in describing select subsets of experimental observations.

The present study is driven by the realization that statistical models that have been used in the interpretation of nuclear multifragmentation data [1, 2, 3, 4, 5] fail to provide a coherent or satisfactory IMF production scenario. Among other things, they fail to overcome the fundamental difficulty of traditional equilibrium-statistical decay models [6, 7] in explaining how IMF production can effectively compete with nucleon and light-charged particle production, when the IMF emission barriers are many tens of MeV high, compared to ≈ 6 MeV for protons. It was the inability of these statistical decay models to explain the IMF production rates that gave rise to the attractive speculation that multiple IMF production could be a manifestation of the liquid-gas phase transition in finite nuclear matter. This is so, because one would expect a gas of nucleons enclosed in a container of sufficiently large size to equilibrate under certain circumstances into a mix of nucleons, light-charged particles, and IMFs. This would be a process essentially analogous to condensation of a gas into liquid droplets. If this were the case, the abundance of IMFs could be large and, perhaps, comparable to that observed experimentally.

For many years, speculations regarding the relevance of the liquid-gas transition for what is termed nuclear multifragmentation have driven studies of this latter phenomenon. So far, however, scrutiny of practical models featuring such a phase transition [2, 3, 4, 5] has revealed significant gaps in the chain of reasoning leading to the “prediction” of an experimentally observable liquid-gas phase transition. For example, models based on the concept of an existence of a freeze-out configuration [3, 4] utilize in their formalisms a “thought” container with ideally reflecting walls, the boundary of the freeze-out volume. Reflection of any outgoing flux of nucleons and light-charged particles (LCP) back into

the freeze-out volume, [8] is crucial for the models allowing particles to eventually form bigger clusters, the intermediate-mass fragments. However, since there is no known physical boundary defining such a freeze-out volume, or mechanism by which IMFs could pass the high saddle of emission barriers, the predicted IMF abundance must be considered an artifact of the modelling itself.

Similarly severe are shortcomings of approaches utilizing percolation [5] or Fisher’s model, [2] which have recently been applied [9] to nuclear multifragmentation. [10] Notably, these models do not even address the issue of the high Coulomb barrier inhibiting fragment emission. The presence of a high barrier is obvious even in the vicinity of the critical point, where the expected matter density (in the range of $1/3 - 1/2$ of ground-state matter density) is still high enough to trap any fragment formed inside the expanded nuclear system in very much the same way as it would trap fragments formed at ground state density. In the case of Fisher’s model, largely overlooked remains the fact that, by design, the formalism is limited to events in which there is no more than one cluster present at any time, with the balance of the system being always in a state of a homogenous, monomeric gas of individual molecules. While such “either-zero-or-one-fragment” events may be essential in a condensation theory, such as represented by Fisher’s model, they are of little, if any, interest in the context of nuclear multifragmentation.

A somewhat different statistical approach to explaining high yields of IMFs observed in energetic nuclear reactions was adopted in the expanding-emitting source model (EESM). [1] This model considers dynamic, isentropic, self-similar expansion of a nuclear system to densities below the equilibrium density proper for the given total excitation energy, where it finds enhanced fragment emission probabilities. However, as pointed out recently, [8] the EESM formalism unjustifiably derives most of the (collective) energy necessary for a fragment to overcome the Coulomb emission barrier, not from a thermal heat bath, as prescribed by Weisskopf’s approach, [11] but from a thermally isolated single, compressional degree of freedom.

The above discussion emphasizes the need for an alternative scenario of statistical IMF emission. The present study demonstrates that a simple scenario, closely related to that known from fission studies, offers an explanation of how at moderately high excitation energies, IMF emission can compete effectively with nucleon evaporation. It represents an extension of ideas and formalism presented in a recent publication. [12] Central to

this formalism is the notion of a relatively high entropy associated with the diffuse nuclear surface region (as opposed to bulk matter). Note that it is also the increased surface entropy that enhances the fission probability of a heavy nucleus relative to nucleon evaporation. This latter enhancement is commonly described in terms of the ratio a_f/a_n of level density parameters for saddle and ground-state configurations, respectively.

The formalism adopted in the present study is described in detail in Section II. While this formalism is somewhat schematic, it is believed to capture the essential physics underlying the processes involved. One benefit of such a schematic treatment is that it provides a direct insight into the phenomena of interest, disregarding a multitude of secondary details demanded by a more rigorous approach. Results of calculations are presented in Section III, while the conclusions are presented in Section IV.

II. THEORETICAL FORMALISM

The present study assumes that an excited nuclear system expands in a self-similar fashion so as to reach a state of approximate thermodynamical equilibrium, where the entropy S is maximal for the given total excitation energy E_{tot}^* , i.e.,

$$\left. \frac{\partial S(E_{tot}^*, \rho)}{\partial \rho} \right|_{E_{tot}^*} = 0. \quad (1)$$

The functional dependence of entropy on E_{tot}^* and the bulk nuclear matter density ρ is evaluated using the Fermi-gas model relationship

$$S = 2\sqrt{aE_{th}^*} = 2\sqrt{a(E_{tot}^* - E_{compr})}, \quad (2)$$

where a is the level density parameter, E_{th}^* is the thermal excitation energy and E_{compr} is the collective compressional energy. The dependence of S on bulk nuclear matter density ρ arises in Eq. 2 through the dependence of both, the level density parameter a (“little- a ”) and the compressional energy E_{compr} on the matter density.

The dependence of little- a on the nuclear matter density for infinite nuclear matter is given by the Fermi-gas model:

$$a = a_o \left(\frac{\rho}{\rho_o} \right)^{-\frac{2}{3}}, \quad (3)$$

where a_o is the level density parameter for the nuclear matter at ground-state matter density ρ_o .

The above equation holds approximately also for finite nuclei if the expansion or compression of these nuclei is assumed to occur in a self-similar fashion. This is so because for finite nuclei, the little- a parameter consists [13, 14] of volume and surface terms, a_V and a_σ , respectively, both of which are proportional to $\rho^{-2/3}$ under the assumption of self-similar expansion:

$$a = a_V + a_\sigma = A\left(\frac{\rho}{\rho_o}\right)^{-\frac{2}{3}}\alpha_V + A^{\frac{2}{3}}\left(\frac{\rho}{\rho_o}\right)^{-\frac{2}{3}}\alpha_\sigma, \quad (4)$$

where α_V and α_σ are volume and surface coefficients, respectively, independent of bulk nuclear matter density.

The term ‘‘self-similar expansion’’ is used here to describe a type of expansion in which any change in the matter density profile is reducible to a simple rescaling of the radial coordinate, such that:

$$f_\rho(r) = c^3 f_o(cr), \quad (5)$$

where $f_o(r)$ is the ground-state density profile function and c is a scaling constant.

The presence of a surface contribution to the level density parameter is of crucial importance in the present study as it describes the part S_σ of entropy S of the system associated with the diffuse surface domain and is seen to have significant effect on the fragment emission probability. One has

$$S = S_V + S_\sigma = a_V T + a_\sigma T, \quad (6)$$

where S_V is the entropy of the bulk matter and T is the system temperature.

The compressional energy in Eq. 2 is approximated in the present study following the schematic prescription proposed in the expanding emitting source model EESM [1], i.e.,

$$\epsilon_{compr} = \epsilon_b \left(1 - \frac{\rho}{\rho_o}\right)^2, \quad (7)$$

where ϵ_{compr} and ϵ_b are the compressional and the ground-state binding energy per nucleon of the system, respectively. Note that Eq. 7 ensures that the compressional energy varies parabolically with ρ , from zero at ground-state density (ρ_o) to ϵ_b at zero density.

Equations 1–3 and 7 allow one to obtain an analytical expression for the equilibrium density, ρ_{eq}/ρ_o , of nuclear matter as a function of the excitation energy per nucleon, $\epsilon_{tot}^* = E_{tot}^*/A$, where A is the mass number of the system:

$$\frac{\rho_{eq}}{\rho_o} = \frac{1}{4} \left(1 + \sqrt{9 - 8 \frac{\epsilon_{tot}^*}{\epsilon_b}} \right). \quad (8)$$

Equation 8 reflects the fact that for $\epsilon_{tot}^* < \epsilon_b$, the system is bound as far as the self-similar expansion mode is concerned, and features a single maximum in entropy in the range of matter densities $1/2 \leq \rho_{eq}/\rho_o \leq 1$. For $\epsilon_{tot}^* \geq \epsilon_b$, the system is essentially unbound with respect to the self-similar expansion mode, with the entropy diverging as the matter density ρ tends to zero. However, for $(9/8)\epsilon_b \geq \epsilon_{tot}^* \geq \epsilon_b$, the system still has a local metastable maximum at a finite density given by Eq. 8, i.e., in the range of matter densities $1/4 \leq \rho_{eq}/\rho_o \leq 1/2$. The latter metastable (with respect to self-similar expansion mode) maximum in entropy is separated from the divergence at zero density by a minimum at ρ_{saddle} , where

$$\frac{\rho_{saddle}}{\rho_o} = \frac{1}{4} \left(1 - \sqrt{9 - 8 \frac{\epsilon_{tot}^*}{\epsilon_b}} \right). \quad (9)$$

Here, $E_b = A\epsilon_b$.

Further, one can obtain the caloric equation of state of an equilibrated system (i.e. at constant, zero external pressure) by using the Fermi-gas model relationship between the system temperature T and thermal excitation energy E_{th}^*

$$T = \sqrt{\frac{E_{th}^*}{a}} = \left(\frac{\rho_{eq}}{\rho_o} \right)^{\frac{1}{3}} a_o^{-\frac{1}{2}} \sqrt{E_{tot}^* - E_b \left(1 - \frac{\rho_{eq}}{\rho_o} \right)^2}. \quad (10)$$

The probability p of emitting a fragment from an equilibrated excited system as defined above can be evaluated using the Weisskopf formalism: [11]

$$p \propto e^{\Delta S} = e^{S_{saddle} - S_{eq}}, \quad (11)$$

where S_{saddle} and S_{eq} are saddle-point and equilibrium-state entropies, respectively. The latter two entropies can be calculated using Eq. 2:

$$S_{eq} = 2 \sqrt{a_A [E_{tot}^* - E_b \left(1 - \frac{\rho_{eq}}{\rho_o} \right)^2]}, \quad (12)$$

$$S_{saddle} = S_{res} + S_{frag} = 2\sqrt{(a_{res} + a_{frag})E_{saddle}^{*th}}. \quad (13)$$

In Eqs. 12 and 13, a_A , a_{res} and a_{frag} are the level density parameters of the system at equilibrium, the residue, and the fragment, respectively, while E_{saddle}^{*th} is the thermal excitation energy of the system in the saddle-point configuration. The latter quantity is calculated as

$$E_{saddle}^{*th} = E_{tot}^* - E_b(1 - \frac{\rho_{eq}}{\rho_o})^2 - V_{saddle}, \quad (14)$$

where V_{saddle} is the (collective) saddle-point energy.

Formally, the emission probability p can be also expressed in terms of an effective emission barrier B_{eff} ,

$$p \propto e^{-\frac{B_{eff}}{T}}, \quad (15)$$

when one sets

$$B_{eff} = -T\Delta S. \quad (16)$$

A selection of results of calculations performed using the above formalism is presented in Section III below.

III. RESULTS OF MODEL CALCULATIONS

Results of the calculations performed in the framework of the formalism presented in Section II are presented in Figs. 1–7. In these calculations, values of $\alpha_V=1/14.6$ MeV⁻¹ and $\alpha_\sigma=4/14.6$ MeV⁻¹ have been assumed for the coefficients α_V and α_σ , as suggested in literature [13]. Further, $\epsilon_b=8$ MeV was assumed [1] for the ground-state binding energy per nucleon, while the saddle-point collective energy was approximated by the Coulomb energy of the residue and fragment represented by two touching spheres of radius parameter $r_{Coul} = 1.3(\rho/\rho_o)^{-1/3}$ fm. The calculations were made for excited ¹⁹⁷Au nuclei.

Fig. 1 illustrates the dependence of the equilibrium density, ρ_{eq} , of bulk matter on the excitation energy per nucleon (solid curve). As seen in this figure, for the range of excitation energies readily accessible in experiments, the bulk matter density in a state of maximum

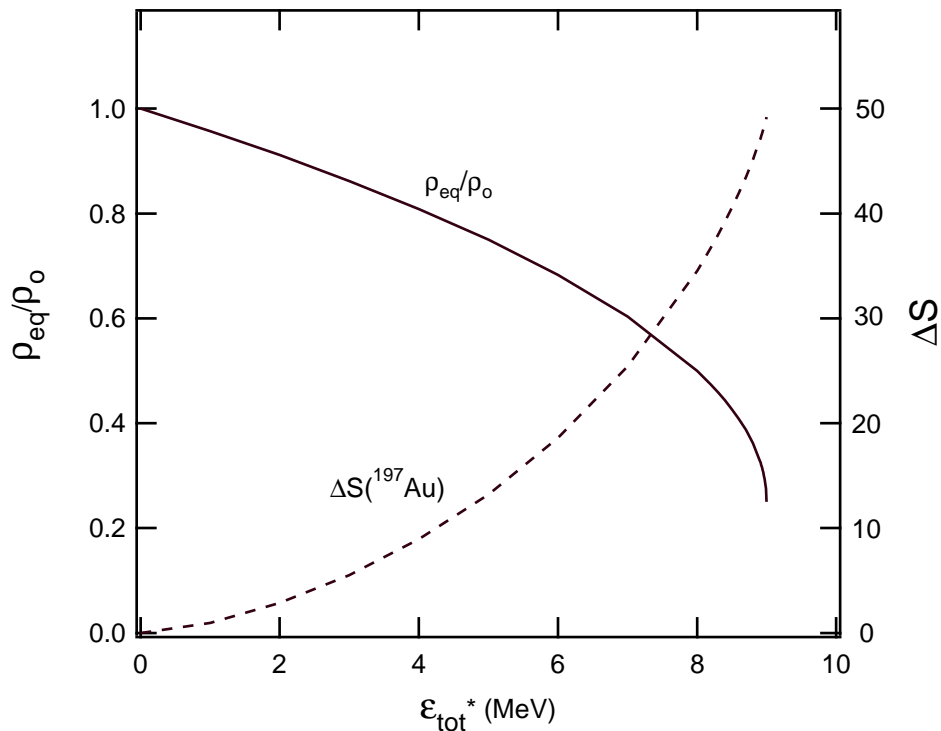


FIG. 1: Equilibrium density of bulk nuclear matter (solid curve) and the net gain in entropy realized by an ^{197}Au system as a result of the relaxation of the self-similar expansion mode (dashed curve), plotted as functions of total excitation energy per nucleon.

entropy differs substantially from that of the nuclear ground state. This affects both, the caloric equation of state and the fragment emission probability, two entities of considerable interest.

The dashed curve seen in Fig. 1 illustrates the net gain in entropy resulting from the relaxation of the self-similar expansion mode in an excited ^{197}Au system. Large gains in entropy associated with the relaxation of this mode emphasize the importance of this mode for a statistical description of excited nuclear systems, notably for models based on the concept of microcanonical [3] or pseudo-microcanonical [4] equilibrium.

The caloric curve calculated for states of maximum entropy, i.e., for the states of equilibrium density ρ_{eq} is depicted in Fig. 2. Not surprisingly, this curve shows considerable deviation from the simple Fermi-gas form of $T \propto \sqrt{E_{tot}^*}$. Note that in experiments, such as the recently reported ISIS experiment, [15] it is E_{tot}^* and not the purely thermal contribution to it, E_{th}^* , that is in fact measured. This is so, because the static compressional energy

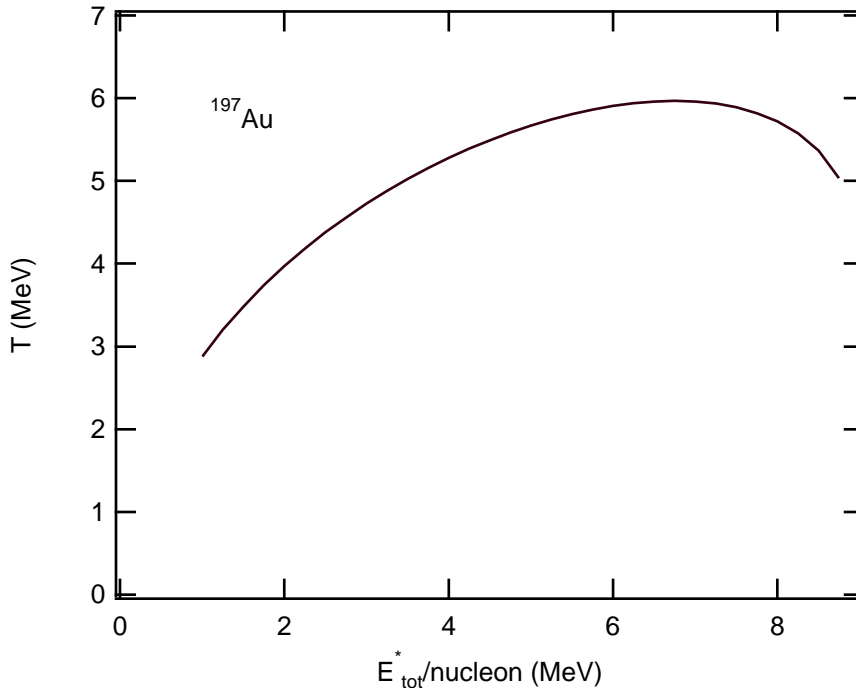


FIG. 2: Caloric curve for the ^{197}Au system.

E_{compr} is experimentally undistinguishable from thermal excitation E_{th}^* .

Most notably, the caloric curve seen in Fig. 2 features a maximum temperature of approximately $T_{max}=6$ MeV, an indication that for higher temperatures the system is inherently unstable and does not find an equilibrium density. In other words, under the assumption that its matter distribution is homogeneous, a nuclear system placed in a heat bath of $T > 6\text{MeV}$ would expand indefinitely, for which it would derive increasing amounts of energy from the heat bath. In a more realistic case, which is beyond the present consideration, the system would likely decay into a “gas” of fragments and free nucleons that would continue its indefinite expansion.

The particular form of the caloric curve seen in Fig. 2 can, perhaps, be better understood when inspecting the dependence of the free energy F on matter density ρ and temperature T , which is illustrated in Fig. 3. The calculations show that, at temperatures below $T \approx 6\text{MeV}$, the free energy as a function of ρ features two equilibrium points, a local minimum and local maximum, where the latter reflects an unstable equilibrium. These two points predicted for any temperature T of less than approximately 6 MeV, correspond to

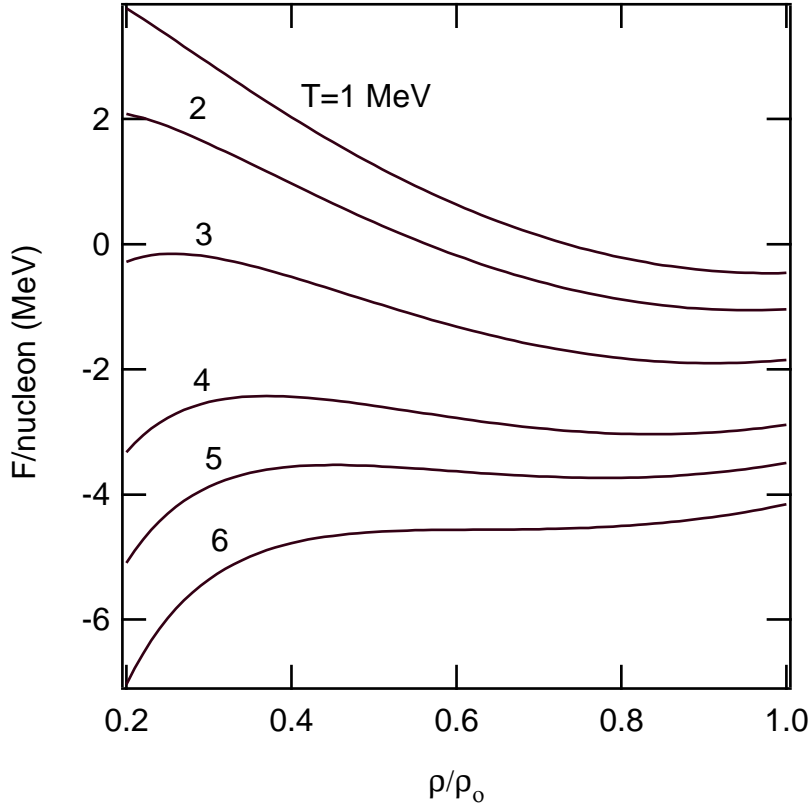


FIG. 3: Free energy for the ^{197}Au system as a function of nuclear matter density and temperature.

different excitation energies per nucleon, ϵ_{tot}^* . Note that at both these extremal points, the pressure of the system at its surface is zero. This is so, because the pressure is proportional to the partial derivative of the free energy with respect to density at constant entropy, and both, the free energy and the entropy are stationary with respect to the matter density at the extremal points in question. At $T \approx 6\text{MeV}$, the minimum and maximum in F as a function of ρ merge into an inflection point and, then, at even higher temperatures, the free energy features only a monotonic decrease with decreasing ρ . The inflection point in F corresponds to maximum in T as a function of E_{tot}^* . Obviously, a monotonic decrease in free energy with decreasing matter density means that no equilibrium density exists for a given temperature.

The role of the surface entropy in fragment emission is clear from Fig. 4 illustrating the dependence of effective barriers (see Eq. 16) for the emission of ^{12}C and ^{16}O from excited ^{197}Au nuclei. Solid lines in this figure illustrate the results obtained when the surface entropy is

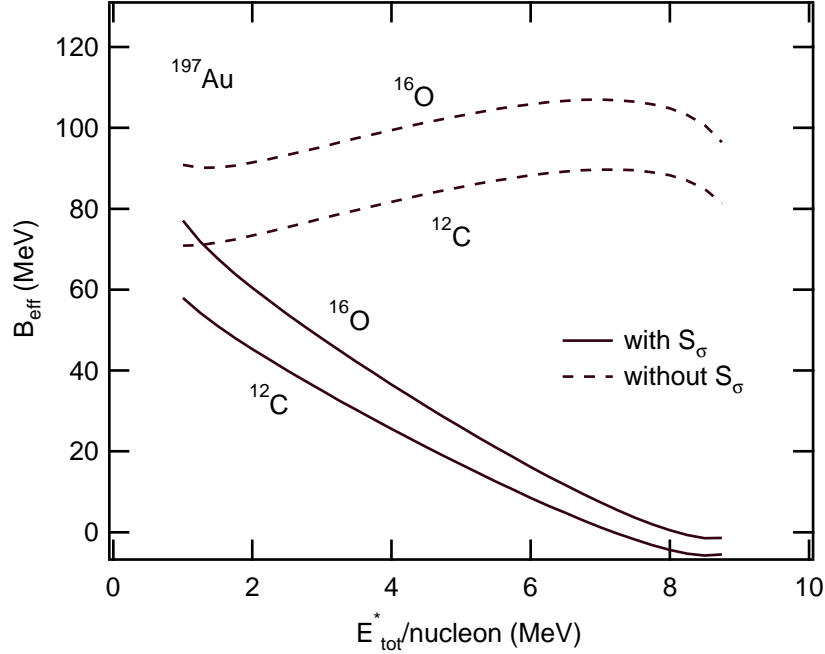


FIG. 4: Effective barriers for the emission of ^{12}C and ^{16}O fragments from equilibrated excited ^{197}Au systems as functions of excitation energy per nucleon.

taken into consideration via inclusion of a_σ in the expression for the level density parameter a (see Eq. 3), while dashed lines represent results of calculations in which the surface entropy effects were neglected, i.e., in which a was assumed simply proportional to the mass number.

It is important to note that with the reduction in the effective barrier being dominantly due to the surface entropy effects, no analogous reduction is expected for the emission of nucleons or light charged particles. In the latter case, the effective barriers are expected to show trends similar to those shown by the dashed lines in Fig. 4.

The effects of the surface entropy on the relative emission rates of various IMFs are illustrated in Fig. 5, displaying the reduced probabilities (taken as bare Boltzmann factors) for the emission of IMFs of different atomic numbers from an equilibrated ^{197}Au system as functions of the total excitation energy per nucleon. The spectra are normalized to the probability for emitting a proton, bound to the system by $Q_p=8$ MeV and experiencing a Coulomb barrier of 4 MeV (corresponding to a Coulomb radius parameter of $r_C=1.3$ fm). As seen in this figure, already at excitation energies per nucleon of the order of 3 MeV/nucleon,

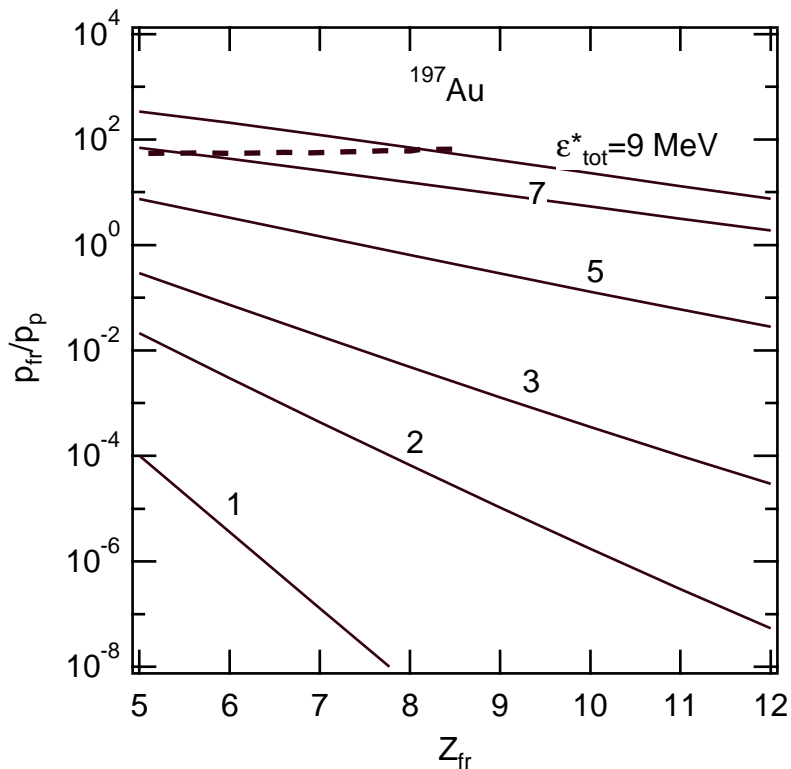


FIG. 5: Distributions of relative emission probabilities of various IMFs from an excited, equilibrated ^{197}Au system as functions of the total excitation energy (solid curves). The dashed line represents the boundary of the domain of dynamical instability of the system. (See text)

fragment emission begins to compete effectively with proton emission and, then, at higher excitation energies, fragment emission becomes the dominant decay mode. Note, that the highest probabilities seen in Fig. 5, above the dashed line, reflect dynamical instability with respect to the fragment emission mode. In fact, Weisskopf's approach [11] is inapplicable in the domain above the dashed line, as in this domain, the saddle-point entropy exceeds that for the “equilibrium” density of a self-similarly expanded system. In the calculations, it was assumed that the mass number of the fragment is twice the atomic number, i.e., $A_{fr} = 2Z_{fr}$.

Since the magnitude of the effective barrier depends on the excitation energy and, thus, on temperature T , and since T is a non-monotonic function of E_{tot}^* , one would expect the fragment emission probabilities p to deviate significantly from a simple Arrhenius law with an exponential functional dependence on the inverse temperature $1/T$. This expectation is confirmed by Fig. 6, where logarithmic plots of p versus $1/T$ are seen to feature clear

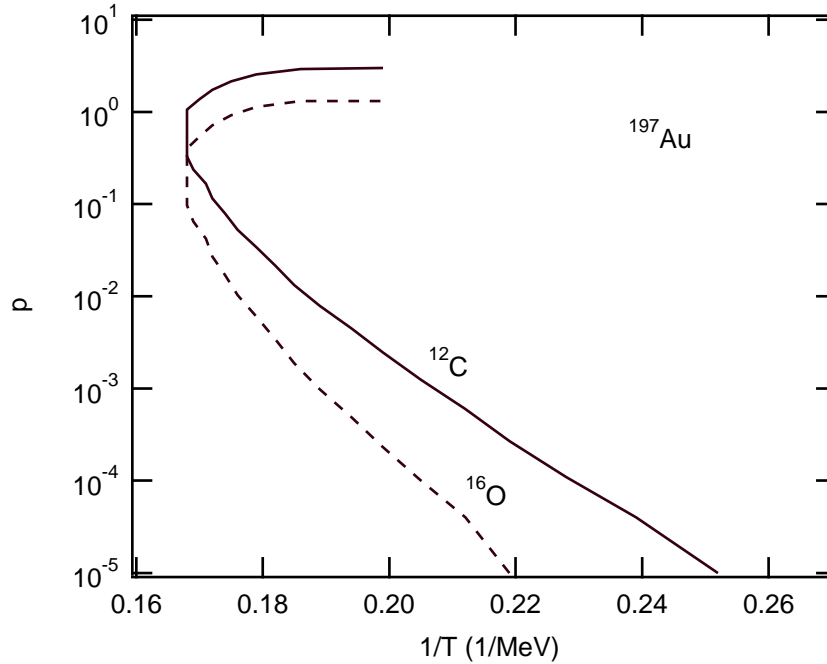


FIG. 6: Arrhenius plots for emission of ^{12}C and ^{16}O fragments from excited ^{197}Au systems.

deviations from linearity, including a prominent “back-bending”. The latter back-bending is obviously expected in view of the maximum in the caloric curve seen in Fig. 2. Such a behavior is also suggested by the general deviation of the caloric equation of state from the one for a low-temperature Fermi gas.

On the other hand, pseudo-Arrhenius plots depicted in Fig. 7, where the logarithm of the emission probability, $\ln(p)$, is plotted *versus* the inverse square root of the total excitation energy, $1/\sqrt{E_{tot}^*}$, are to a good approximation straight lines. This observation comes as a surprise, as it cannot readily be expected based on the details of the theoretical formalism employed. Therefore, no simple explanation for such a linearity can be offered at this time, the very rationale behind the construction of such pseudo-Arrhenius plots being numerous experimental findings. [9, 16, 17, 18, 19] While it may be purely fortuitous, the linear character of pseudo-Arrhenius plots predicted by the present formalism seems to be in agreement with experimental observations.

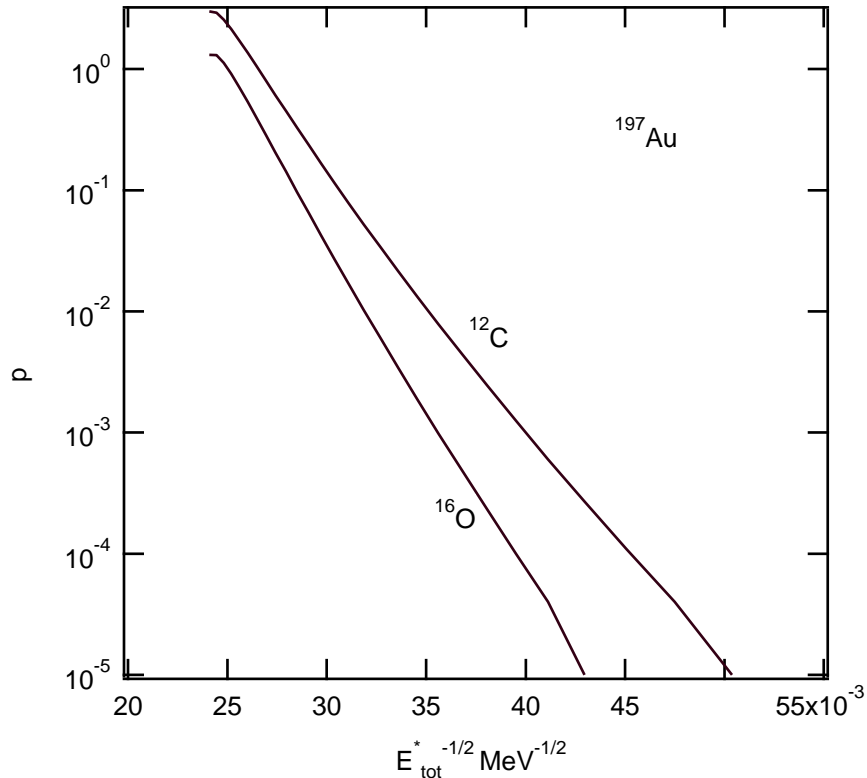


FIG. 7: Pseudo-Arrhenius plots for emission of ^{12}C and ^{16}O fragments from excited ^{197}Au systems.

IV. CONCLUSIONS

A formalism has been developed to describe quantitatively, albeit in a schematic fashion, a scenario of purely statistical emission of massive fragments from finite equilibrated systems. The formalism recognizes the importance of thermal expansion of hot matter and considers the stability of such systems at equilibrium nuclear densities. The important role of surface entropy consists in an effective “softening” of the nuclear surface, resulting in enhanced fragment emission probabilities. The decay scenario underlying this formalism is that of a thermally expanded system with developed thermal fluctuations of the diffuse surface. Within such a scenario, fragment emission is naturally viewed as analogous to fission.

The calculations performed within the framework of the proposed formalism show that, with increasing excitation energy and mostly due to effects of increased surface entropy, the effective barriers for fragment emission decrease and, eventually, vanish. As no equivalent decrease is expected for nucleons and light charged particles, one expects that at high

excitation energies, fragment emission competes effectively with nucleon and LCP emission.

The formalism presented here also predicts an occurrence of negative heat capacity in highly excited nuclear systems. It also predicts linear pseudo-Arrhenius plots, where the logarithm of the fragment emission probability, $\ln(p)$, is plotted *versus* the inverse square-root of the excitation energy, $1/\sqrt{E^*}$. This latter prediction is found in agreement with numerous experimental observations. [16, 17, 18, 19] However, as also expected, the formalism predicts non-linear true Arrhenius plots, where the independent variable is the inverse temperature, $1/T$, rather than $1/\sqrt{E^*}$. This is so, because the effective emission barriers depend rather strongly on excitation energy (and temperature) and, hence, fail to satisfy one of the fundamental prerequisites of the Arrhenius law.

The simplicity of the presented formalism should allow one to incorporate it into existing statistical decay codes. For purposes where the ultimate goal is to obtain an agreement with experimental data, it would be desirable, however, to improve the formalism itself. For example, one should use more realistic (and lower) saddle-point energies, instead of the schematic Coulomb energies of touching spheres. One should also be mindful of differences in equilibration times for nucleon and LCP emission modes, on the one hand, and for different IMF emission and fission modes, on the other hand. It is natural to expect that modes requiring major rearrangement of mass require longer times to equilibrate than modes that do not require such a rearrangement. Consequently, one would expect all IMF emission modes to attain equilibrium later than nucleon emission modes, and fission modes to reach equilibrium even later. As a result, early in the decay process, while the IMF degree of freedom is approaching equilibrium, one would expect to see “pre-IMF nucleons”, in much the same way as one sees pre-fission neutrons. [20, 21] Similarly, one would expect to see pre-fission IMF emission in situations when for the same systems at equilibrium, fission would dominate. Importantly, the latter pre-fission IMF emission modes may succeed in removing enough charge and excitation energy from the system so as to pre-empt fission altogether - a phenomenon that has recently been observed experimentally. [22]

Acknowledgments

This work was supported by the U.S. Department of Energy grant No. DE-FG02-88ER40414.

- [1] W. A. Friedman, Phys. Rev. Lett. **60**, 2125 (1988).
- [2] M. E. Fisher, Physics (N.Y.) **3**, 255 (1967).
- [3] D. H. E. Gross, Phys. Rep. **279**, 119 (1997).
- [4] J. P. Bondorf et al., Phys. Rep. **257**, 133 (1995).
- [5] W. Bauer, Phys. Rev. C **38**, 1297 (1988).
- [6] R. J. Charity, Computer code Gemini, wunmr.wustl.edu/pub/gemini.
- [7] A. Gavron, Phys. Rev. C **21**, 230 (1980).
- [8] J. Töke, Nucl. Phys. **A681**, 6374c (2001).
- [9] L. G. Moretto, L. Phair, and G. J. Wozniak, Phys. Rev. C **60**, R031601 (1999).
- [10] J. Schmelzer, G. Röpke, and R. Mahnke, *Aggregation Phenomena in Complex Systems* (Wiley–VCH, Weinheim, 1999), p. 263.
- [11] V. F. Weisskopf, Phys. Rev. **52**, 295 (1937).
- [12] J. Töke and W. U. Schröder, Phys. Rev. Lett. **82**, 5008 (1999).
- [13] J. Töke and W. J. Swiatecki, Nucl. Phys. A **372**, 141 (1981).
- [14] A. V. Ignatyuk et al., Sov. J. Nucl. Phys. **21**, 612 (1975).
- [15] L. Beaulieu et al., Phys. Rev. **C63**, 031302 (2001).
- [16] L. G. Moretto et al., Phys. Rev. Lett. **74**, 1530 (1995).
- [17] K. Tso et al., Phys. Lett. **361**, 25 (1997).
- [18] L. G. Moretto et al., Phys. Rep. **287**, 249 (1997).
- [19] L. Beaulieu, L. Phair, L. G. Moretto, and G. J. Wozniak, Phys. Rev. Lett. **81**, 770 (1998).
- [20] D. Hilscher and H. Rossner, Ann. Phys. Fr. **17**, 471 (1992).
- [21] D. J. Hinde et al., Phys. Rev. C **45**, 1229 (1992).
- [22] B. Djerroud et al., Phys. Rev. C **64**, 034603 (2001).